0026-895X/01/5904-732–743$3.00
MOLECULAR PHARMACOLOGY
Copyright © 2001 The American Society for Pharmacology and Experimental Therapeutics
Mol Pharmacol 59:732–743, 2001

Vol. 59, No. 4
496/891505
Printed in U.S.A.

Modulation of Neuronal Nicotinic Acetylcholine Receptors by Halothane in Rat Cortical Neurons

TAKASHI MORI, XILONG ZHAO, YI ZUO, GARY L. AISTRUP, KIYONOBU NISHIKAWA, WILLIAM MARSZALEC, JAY Z. YEH, and TOSHIO NARAHASHI

Department of Molecular Pharmacology and Biological Chemistry, Northwestern University Medical School, Chicago, Illinois

Received August 17, 2000; accepted December 22, 2000

This paper is available online at http://molpharm.aspetjournals.org

ABSTRACT

Inhalational general anesthetics have recently been shown to inhibit neuronal nicotinic acetylcholine (ACh) receptors (nnAChRs) expressed in *Xenopus laevis* oocytes and in molluscan neurons. However, drug actions on these systems are not necessarily the same as those seen on native mammalian neurons. Thus, we analyzed the detailed mechanisms of action of halothane on nnAChRs using rat cortical neurons in long-term primary culture. Currents induced by applications of ACh via a U-tube system were recorded by the whole-cell, patch-clamp technique. ACh evoked two types of currents, α-bungarotoxin-sensitive, fast desensitizing (α7-type) currents and α-bungarotoxin-insensitive, slowly desensitizing ($\alpha4\beta2$-type) currents. Halothane suppressed $\alpha4\beta2$-type currents more than α7-type currents with IC_{50} values of 105 and 552 μM, respectively. Halothane shifted the ACh dose-response curve for the $\alpha4\beta2$-type currents in the direction of lower ACh concentrations and slowed its apparent rate of desensitization. The rate of recovery after washout from halothane block was much faster than the rate of recovery from ACh desensitization. Thus, the halothane block was not caused by receptor desensitization. Chlorisondamine, an irreversible open channel blocker for nnAChRs, caused a time-dependent block that was attenuated by halothane. These results could be accounted for by kinetic simulation based on a model in which halothane causes flickering block of open channels, as seen in muscle nAChRs. Halothane block of nnAChRs is deemed to play an important role in anesthesia via a direct action on the receptor and an indirect action to suppress transmitter release.

Inhalational anesthetics induce a wide spectrum of clinical effects such as unconsciousness, amnesia, analgesia, muscle relaxation, attenuation of protective reflex, and hemodynamic suppression (Kissin, 1993; Stanski, 1994). These diverse effects could reflect an integration of separate pharmacological actions of anesthetics (Kissin, 1993). Ever since anesthetic potency was shown to correlate with the lipophilicity (Meyer, 1899), perturbation of the membrane lipid has been hypothesized as a cause of general anesthesia. In the past decade, however, there has been increasing evidence for the membrane proteins to be a target of general anesthetics (Franks and Lieb, 1994). Inhalational anesthetics have been demonstrated to modulate $GABA_A$, glycine, 5-hydroxytryptamine$_3$, and nicotinic acetylcholine receptors (nAChRs) (Franks and Lieb, 1994).

The inhibitory $GABA_A$ receptor has been considered a potential target site for anesthetics because clinically relevant concentrations of inhalational anesthetics potentiate its response (Nakahiro et al., 1989; Yeh et al., 1991). Inhibition of neuronal nAChRs (nnAChRs) by inhalational anesthetics was also found in molluscan neurons (McKenzie et al., 1995). Recently, nnAChRs expressed in *Xenopus laevis* oocytes have been shown to be potently blocked by inhalational anesthetics (Violet et al., 1997; Flood et al., 1997; Cardoso et al., 1999). The rat $\alpha4\beta2$ or $\alpha3\beta2$ subunits of nnAChRs expressed in *X. laevis* oocytes are 20 to 30 times more sensitive to halothane and isoflurane than the muscle nAChRs (Violet et al., 1997). Isoflurane inhibited the $\alpha4\beta2$ subunits with an IC_{50} value of 85 μM but did not inhibit α7 subunits of nnAChRs expressed in *X. laevis* oocytes (Flood et al., 1997). Although inhalational anesthetics inhibited nnAChRs expressed in *X. laevis* oocytes, the structurally related nonimmobilizing compound, F6 or 1,2-dichlorohexafluorocyclobutane, did not (Cardoso et al., 1999). However, it remains to be seen whether anesthetics inhibit the nnAChRs in mammalian native neurons in the central nervous system. It should be pointed out that the pharmacological responses of recombinant receptors expressed in various systems are not necessarily the same as those of native neurons (Cooper and Millar, 1997; Lewis et al., 1997; Sivilotti et al., 1997).

nAChRs consist of pentameric oligomers and an ion channel that is ACh-gated and cation-selective. Neuronal nAChRs differ from skeletal muscle nAChRs (which consist of

This work was supported by National Institutes of Health Grants AA07836 and NS14144.

ABBREVIATIONS: GABA, γ-aminobutyric acid; nAChR, nicotinic acetylcholine receptors; nnAChRs, neuronal nicotinic acetylcholine receptors; ACh, acetylcholine; α-BuTX, α-bungarotoxin; MAC, minimum alveolar concentration.

$\alpha 1\beta 1\delta\gamma/\epsilon$) and *Torpedo californica* electric organ nAChRs in subunit composition, pharmacology, and biophysical profile (McGehee and Role, 1995; Lindstrom, 1996) and consist of various combinations of subunits ($\alpha 2$-$\alpha 9$, $\beta 2$-$\beta 4$) (McGehee and Role, 1995; Colquhoun and Patrick, 1997b). $\alpha 7$, $\alpha 8$, and $\alpha 9$ subunits form functional and homo-oligomeric receptors, whereas other α subunits form functional receptors only when combined with β subunits (McGehee and Role, 1995; Colquhoun and Patrick, 1997b).

nnAChRs are found in the presynaptic, preterminal, and postsynaptic locations; those at the first two locations render nnAChRs the ability to modulate the release of a variety of neurotransmitters including dopamine, norepinephrine, GABA, glutamate, and ACh itself (Role and Berg, 1996; Alkondon et al., 1997, 1999; Wonnacott, 1997). In addition, ACh is one of the important neurotransmitters released from the brain stem, hypothalamus, basal forebrain, and cerebral cortex that participate in cognition, memory, alertness, learning, and antinociception (Lindstrom, 1997; McCormick and Bal, 1997; Changeux et al., 1998; Marubio et al., 1999). Therefore, the high sensitivity of nnAChRs to inhalational anesthetics suggests that they mediate anesthetic actions such as unconsciousness, drowsiness, amnesia, and cognitive and psychomotor impairment through modulation of the release of various neurotransmitters.

We now report the effects of halothane on nnAChRs in rat cortical neurons in long-term primary culture using the whole-cell, patch-clamp technique. Cortical neurons in culture exhibit two distinct types of ACh-induced currents, α-bungarotoxin (α-BuTX)-sensitive currents and α-BuTX-insensitive currents (Aistrup et al., 1999; Marszalec et al., 1999). The predominant subunits of α-BuTX-sensitive and α-BuTX-insensitive receptors are generally thought to be composed of $\alpha 7$ and $\alpha 4\beta 2$ subunits, respectively (Albuquerque et al., 1997; Changeux et al., 1998). The present study shows that halothane inhibits both α-BuTX-sensitive, $\alpha 7$-type and α-BuTX-insensitive, $\alpha 4\beta 2$-type currents at clinically relevant concentrations. However, $\alpha 4\beta 2$-type currents were more sensitive to halothane than $\alpha 7$-type currents. Therefore, the mechanisms that underlie the halothane inhibition of $\alpha 4\beta 2$-type nnAChRs were investigated in detail.

Materials and Methods

Cell Preparations. Rat cortical neurons were isolated and cultured by a procedure slightly modified from that described elsewhere (Marszalec and Narahashi, 1993). In brief, fetuses were removed from a 17-day pregnant Sprague-Dawley rat under methoxyflurane anesthesia. Small wedges of frontal cortex were excised and subsequently incubated in phosphate-buffered saline solution containing 0.25% (w/v) trypsin (Type XI; Sigma-Aldrich, St. Louis, MO) for 20 min at 37°C. The digested tissue was then mechanically triturated by repeated passages through a Pasteur pipette, and the dissociated cells were suspended in neurobasal medium with B-27 supplement (Life Technologies, Gaithersburg, MD) and 2 mM glutamine. The cells were added to 35-mm culture wells at a concentration of 100,000 cells/ml. Each well contained five 12-mm coverslips (previously coated with poly-L-lysine) overlaid with confluent glia that had been plated 2 to 4 weeks earlier. The cortical neuron/glia coculture was maintained in a humidified atmosphere of 90% air/10% CO_2 at 37°C. Cells cultured for 2 to 9 weeks were used for electrophysiological experiments.

Solutions for Current Recording. The external solution contained 150 mM NaCl; 5 mM KCl; 2.5 mM $CaCl_2$; 1 mM $MgCl_2$; 5.5 mM HEPES acid; 4.5 mM HEPES sodium; and 10 mM D-glucose. Tetrodotoxin (0.1 μM) was added to eliminate sodium channel currents, and atropine sulfate (20 nM) was added to block muscarinic ACh responses. The pH was adjusted to 7.3 and the osmolality was adjusted to 300 mOsmol by D-glucose. The internal solution contained 140 mM potassium-gluconate; 2 mM $MgCl_2$; 1 mM $CaCl_2$; 10 mM HEPES acid; 10 mM EGTA; 2 mM ATP-Mg^{2+}; and 0.2 mM GTP-Na^+. The pH was adjusted to 7.3 with KOH and the osmolality was adjusted to 300 mOsmol by adding D-glucose.

ACh (Sigma) was first dissolved in distilled water to make stock solution. Halothane (Fluothane) was obtained from Ayerst Laboratories (New York, NY). Saturated halothane solutions were made by stirring halothane in the external solution over 8 h in a sealed glass container with very little air space. Halothane test solutions were prepared immediately before experiments by dilution of the saturated solution and were kept in air-free, closed glass bottles to prevent evaporation of halothane. Using ^{19}F-NMR spectroscopy (GE NMR Instruments), the saturated solution was found to contain 18.0 mM halothane, a value identical with that determined previously (Seto et al., 1992). Taking into account the solubility of halothane (Smith et al., 1981) and temperature (T) (Franks and Lieb, 1993), the aqueous effective concentration for 50% effect (EC_{50}) in rat neurons (Franks and Lieb, 1996) was estimated by the equation $EC_{50}|_{T(°C)} = \exp[(-4.08 \times (37 - T))/(273.15 + T)] \times EC_{50}|_{37°C}$. The concentration of halothane in aqueous phase at 22°C (0.25 mM) is very close to 0.23 mM in equilibrium with 0.4% halothane in air, which corresponds to one minimum alveolar concentration (MAC) for rat (1.03% at 37°C). The concentrations of halothane used in the present experiments were 7.5 to 2500 μM.

Current Recordings. The whole-cell, patch-clamp technique (Hamill et al., 1981) was used to record ionic currents induced by ACh application through a U-tube system. Recording pipettes were pulled in two stages on a vertical pipette puller (PP-83; Narishige, Tokyo, Japan). The pipettes with a relatively large tip diameter (electric resistance 2–3 MΩ when filled with pipette solution) were used to facilitate the diffusion of pipette solution into the cell. Recording was started about 5 to 10 min after rupture of the membrane under the pipette tip to adequately equilibrate the cell interior with pipette solution. The currents were recorded with a patch-clamp amplifier (Axopatch-1B; Axon Instruments, Foster City, CA) and the membrane potential was held at −70 mV. The experiments were performed at room temperature (22 ± 2°C).

ACh-induced currents were filtered at 5 kHz and digitized at 1 to 10 kHz via a Digidata 1200 analog-to-digital/digital-to-analog converter interfaced to a microcomputer under control of the ClampEx module of the PClamp6 software package (Axon Instruments).

Drug Application. The speed of the U-tube system (Marszalec and Narahashi, 1993) had a rise time of 60 ms as measured by a change in junctional potential with a patch electrode and the solution exchange near the cell surface was complete within 200 ms, as assessed by the method of Liu and Dilger (1991). A computer-operated magnetic valve controlled this system. In the present study, the term "coapplication" is referred to as the simultaneous application of halothane with ACh through the U-tube only, whereas the term "preperfusion" is referred to as the application of halothane through the external bathing solution. Specific protocols for drug application are given in the respective *Results* subsections.

Analyses. Current records were initially analyzed via the ClampFit module of the PClamp6 to assess whole-cell current amplitude and decay kinetics. ACh concentration-response data and anesthetic inhibition data were fitted to the sigmoidal logistic equation (Hill equation) using the SigmaPlot (SPSS Science, Chicago, IL). Data were expressed as mean ± S.D. unless otherwise stated. Analyses of variance and/or Student's t tests were performed to assess significance of differences, if applicable. P values less than 0.05 were considered statistically significant.

Simulation. The kinetic simulation was carried out with a C++ program for numerical solution for the conducting channel according

to simplified schemes for halothane to modulate dose-response relationships and desensitization induced by ACh, and open channel block by chlorisondamine.

Results

Morphology and conditions of rat cortical neurons in long term culture were described elsewhere (Aistrup et al., 1999). Briefly, after 2 weeks in culture, neurons projected their neurites and established complex network. This was evidenced by spontaneous activity recorded as excitatory and/or inhibitory postsynaptic currents, primarily mediated by *N*-methyl-D-aspartate and GABA receptors, respectively (Marszalec et al., 1998). After about 3 weeks, neurons began to express nnAChRs to generate ACh-induced currents. The properties of ACh-induced currents observed in rat cortical neurons were examined and described in our previous article (Aistrup et al., 1999). ACh induced two distinct types of currents differing in pharmacology and decay kinetics. One is an α-BuTX-sensitive current that exhibits fast desensitization and another is an α-BuTX-insensitive current that exhibits slow desensitization. These two types of current are generally thought to be mediated by α7-type and $\alpha4\beta2$-type nnAChRs, respectively. In some cells, a mixture of α7-type and $\alpha4\beta2$-type currents was observed.

The effects of halothane on ACh-induced currents were examined using the following protocol unless otherwise stated. ACh and halothane were coapplied through a U-tube, and halothane was perfused through the bath starting 2 min before the coapplication. Two-minute preperfusion was long enough to exchange the whole bath solution and to allow halothane to exhibit maximal effect.

Halothane Inhibition of Mixed α7-Type and $\alpha4\beta2$-Type Currents. The effect of halothane on neurons exhibiting both α7-type and $\alpha4\beta2$-type currents (Fig. 1A) was studied first. Halothane at 250 μM inhibited the mixed type current (Fig. 1B). After washout of halothane, 25 nM α-BuTX perfused in the bath blocked the α7-type, fast component of current without affecting $\alpha4\beta2$-type, slow component of current (Fig. 1C). Halothane at 250 μM inhibited the $\alpha4\beta2$-type currents (Fig. 1D). However, the α7-type currents estimated by subtracting current of C from A and D from B were only slightly inhibited by halothane (Fig. 1, E and F). This experiment clearly showed that halothane inhibited $\alpha4\beta2$-type currents more potently than α7-type currents. In the following experiments, the effects of halothane on α7-type and $\alpha4\beta2$-type currents were examined separately.

Halothane Inhibition of α7-Type Currents. To record α7-type currents, we tried to find cells that exhibited no $\alpha4\beta2$-type currents. The concentration-dependent effect of halothane was examined at an ACh concentration of 300 μM, which is near the EC_{50} value for α7-type currents. Halothane inhibited α7-type currents reversibly in a concentration-dependent manner (Fig. 2A). The IC_{50} and Hill coefficient obtained from the halothane inhibition curve were 552 μM and 2.45, respectively (Fig. 2B). This concentration of halothane is clinically relevant but is twice as high as the MAC.

The effect of halothane on the ACh concentration-response curve of α7-type currents was tested at a concentration of 750 μM. Halothane inhibited α7-type currents at all ACh concentrations tested ranging from 100 μM to 3 mM (Fig. 3A). This inhibition was independent of ACh concentration. The ACh EC_{50} values before and after halothane application were 267 to 259 μM, respectively, and the Hill coefficients were 1.18 and 1.04, respectively (Fig. 3B), indicating that halothane inhibition of α7-type currents is noncompetitive in nature.

The decay phase of α7-type current was accelerated by halothane. When the amplitudes of currents recorded in the absence and presence of halothane (500 μM) were normalized (Fig. 4A), a slight acceleration of the decay phase by halothane was noted (Fig. 4A). The decay phase could be fitted by a single exponential function. Halothane at concentrations of 250, 500, and 750 μM reduced the decay time constant in a concentration-dependent manner and at ACh concentrations of 30 μM to 3 mM (Fig. 4, B and C). This suggests that halothane either accelerates the desensitization or blocks open channel.

Halothane Effect on $\alpha4\beta2$-Type Currents. To isolate $\alpha4\beta2$-type currents, α-BuTX (25 nM) was applied in the bath to block α7-type currents. The concentration-dependent effect of halothane on $\alpha4\beta2$-type currents was examined at an ACh concentration of 300 μM, which caused the maximum response. Halothane inhibited $\alpha4\beta2$-type currents in a concentration-dependent manner at clinically relevant concentrations (Fig. 5A). The inhibition was reversible after washout of halothane. The IC_{50} and Hill coefficient obtained from

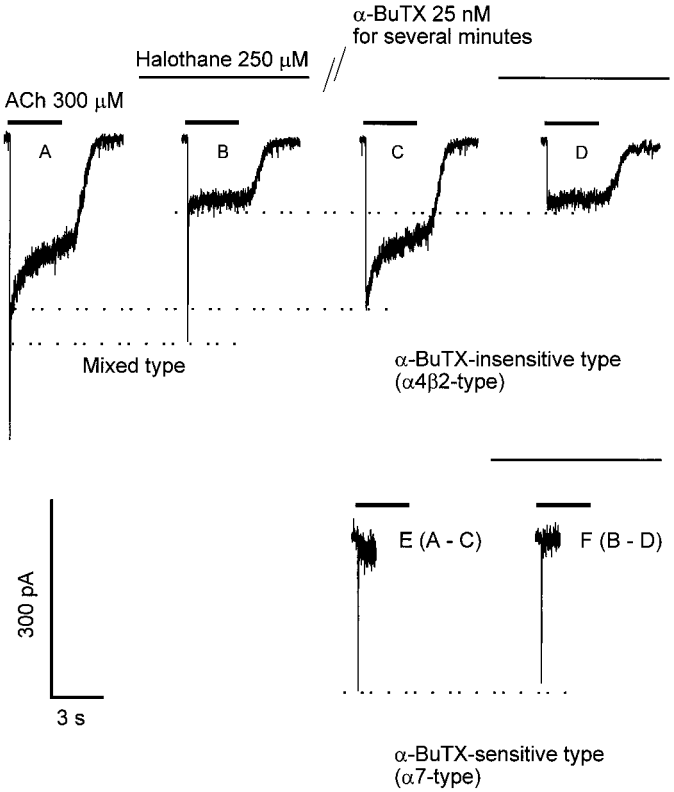

Fig. 1. Differential sensitivity of α7-type and $\alpha4\beta2$-type currents to halothane. To induce currents, ACh (300 μM) was applied through a U-tube for 3 s (thick horizontal bar). Halothane 250 μM was preperfused 2 min before the test ACh pulse and was also coapplied with ACh (thin horizontal bar). A, A mixture of α7-type and $\alpha4\beta2$-type currents. B, halothane inhibited the mixed current. C, α-BuTX blocked α7-type current without affecting $\alpha4\beta2$-type current. D, halothane inhibited $\alpha4\beta2$-type current. E and F, α7-Type currents were separated by subtracting C from A (E) as the control, and D from B (F) as the current in halothane. The α7-type current was only slightly inhibited by halothane. This clearly shows that halothane inhibits $\alpha4\beta2$-type current more potently than α7-type current.

halothane inhibition curve were 105 μM and 1.1, respectively (Fig. 5B). This IC_{50} value was less than half of the MAC. Therefore, $\alpha4\beta2$-type currents were highly sensitive to halothane and much more sensitive than $\alpha7$-type currents.

The effect of halothane on ACh concentration-response curve of $\alpha4\beta2$-type currents was tested at a halothane concentration of 100 μM. Halothane inhibited the currents at all ACh concentrations tested ranging from 0.3 μM to 1 mM (Fig. 6A). The inhibition was ACh concentration-dependent, being larger at higher concentrations of ACh. Consequently, halothane reduced the ACh EC_{50} value from 5.46 to 1.53 μM and increased the Hill coefficient from 0.61 to 0.99 (Fig. 6B). A shift in ACh dose-response curve toward the direction of lower ACh concentrations and an increase in the Hill coefficient by halothane are consistent with its open channel blocking action. A simulation from such a model will be given later under *Discussion*.

The effect of halothane on the decay phase of $\alpha4\beta2$-type currents was also examined. Because $\alpha4\beta2$-type currents exhibited slow desensitization, ACh was applied for as long as 25 s. In the presence of halothane at 75 μM, the current was reversibly reduced (Fig. 7A). To clarify the difference in the decay phase, the peak current recorded in the presence of halothane was normalized to control peak current (Fig. 7A). The decay phase could be well fit with double exponential functions, and halothane increased both fast and slow decay time constants significantly (Fig. 7B). Thus, the decay phase of $\alpha7$-type and $\alpha4\beta2$-type currents was differentially affected by halothane.

Time Course of Halothane Block of the Activated and Resting $\alpha4\beta2$-Type Receptors. Two protocols were used to monitor the time course of halothane block of ACh-induced currents of $\alpha4\beta2$-type receptors. The protocol to monitor halothane block of the resting $\alpha4\beta2$-type receptors is shown in Fig. 8. Two 1 mM ACh pulses were applied from Picospritzer II (General Valve Corporation, Fairfield, NJ) to generate test currents whereas halothane was applied for 4 s from a U-tube onto the cell. Halothane was washed out between each set of trials. The time to first test pulse from the beginning of halothane application was varied in each trial, and a second pulse was applied 2 s after the onset of halothane application. Plot of the amplitude of the first pulse current as a function of the period of halothane perfusion shows that halothane inhibition of the resting $\alpha4\beta2$-type receptor is time dependent with a time constant of 218 $\pm$ 18 ms (Fig. 8B). Each ▲ in Fig. 8B represents the amplitude of the second pulse current in each trial showing almost a

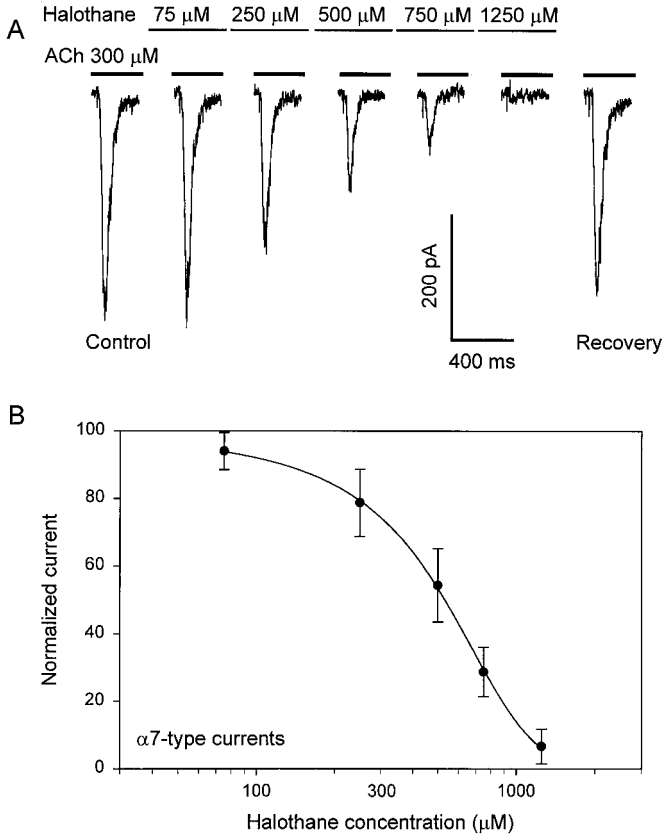

Fig. 2. Halothane block of $\alpha7$-type currents. A, halothane inhibited the currents induced by 300 μM ACh in a concentration-dependent manner. The inhibition was reversible after washout of halothane. B, concentration-response curve for halothane inhibition. The data points are the mean peak currents expressed as percentages of control current, and the error bars are standard deviations (n = 5). The line is unweighted least-squares fit of the data to a Hill equation. The IC_{50} and Hill coefficient obtained from halothane inhibition curve were 552 $\pm$ 52 μM and 2.45 $\pm$ 0.50, respectively.

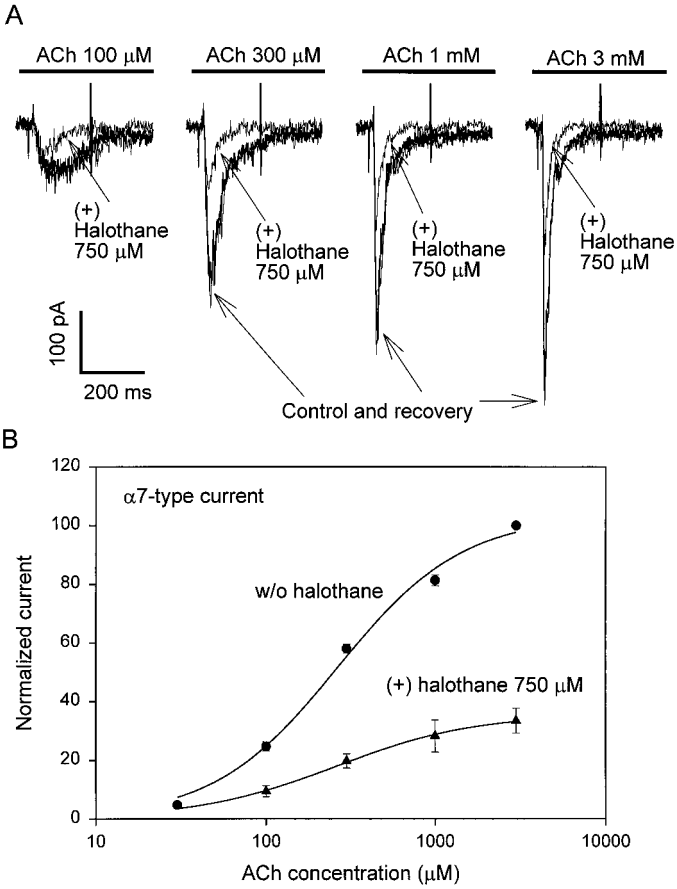

Fig. 3. Halothane block of $\alpha7$-type currents as a function of ACh concentration. A, halothane 750 μM inhibited $\alpha7$-type currents at all ACh concentrations tested. The inhibition was independent of ACh concentration. B, ACh concentration-response curves in the absence and presence of 750 μM halothane. The data points are the mean peak currents expressed as percentages of control current, and the error bars are standard deviations (n = 5). The lines are unweighted least-squares fit of the data to a Hill equation. The ACh EC_{50} and Hill coefficient were not changed by halothane (from 267 $\pm$ 51 μM to 259 $\pm$ 34 μM and from 1.18 $\pm$ 0.20 to 1.04 $\pm$ 0.12, respectively).

constant amplitude, which represents a constant steady-state block. Halothane essentially reached the steady-state block of the resting receptors within 1 s.

The protocol to examine an interaction of halothane with the activated receptor is illustrated in Fig. 9. Three currents recorded from the same cell and induced by 300 μM ACh are superimposed. Control current was recorded in the absence of halothane. Current 1 was induced by coapplication of 250 μM halothane and ACh. Current 2 was induced by ACh when 250 μM halothane was preperfused in the bath and also coapplied with ACh. The current reduction observed with combined preperfusion and coapplication of halothane (current 2) represents the resting receptor block because the receptor was not activated during halothane preperfusion. When halothane was coapplied with ACh without preperfusion, the current exhibited time-dependent decay. If the current decay in the presence of halothane mainly reflects the time course of open channel block, the decay time constant was estimated to be approximately 300 ms in the presence of 250 μM halothane. Because the steady-state level after coapplication of halothane (current 1) reaches the same level as that achieved by a combination of preperfusion and coapplication (current 2), halothane has an identical affinity for both the activated and the resting receptors.

Comparison of Time Course of Recovery from Halothane Block with Desensitized $\alpha4\beta2$-Type Receptors. To assess whether halothane inhibition of $\alpha4\beta2$-type currents was caused by receptor desensitization, the recovery of current from halothane block was compared with the recovery from the ACh-induced desensitization. The time course of recovery from halothane block was examined by two protocols. One is to assess the recovery in the resting state of receptors as shown in Fig. 10. ACh (3 mM) was applied from Picospritzer II as test pulse while halothane was applied in the bath. To observe recovery from resting block, halothane was washed out by halothane-free solution from a U-tube. The time to the first test pulse from the beginning of washout was varied in each set of trial. The second pulse and the third pulse were applied 2 and 3 s after the onset of washout, respectively. Plot of the peak amplitude of the first current as a function of the period of halothane washout shows that halothane recovered from inhibition of the resting receptor with a time constant of 499 $\pm$ 68 ms (Fig. 10).

Fig. 11A shows another protocol used to measure the time course of recovery from halothane block in the activated receptors. Three currents activated by 300 μM ACh are superimposed. Current 1 was generated when halothane was only preperfused for 2 min before ACh test pulse devoid of

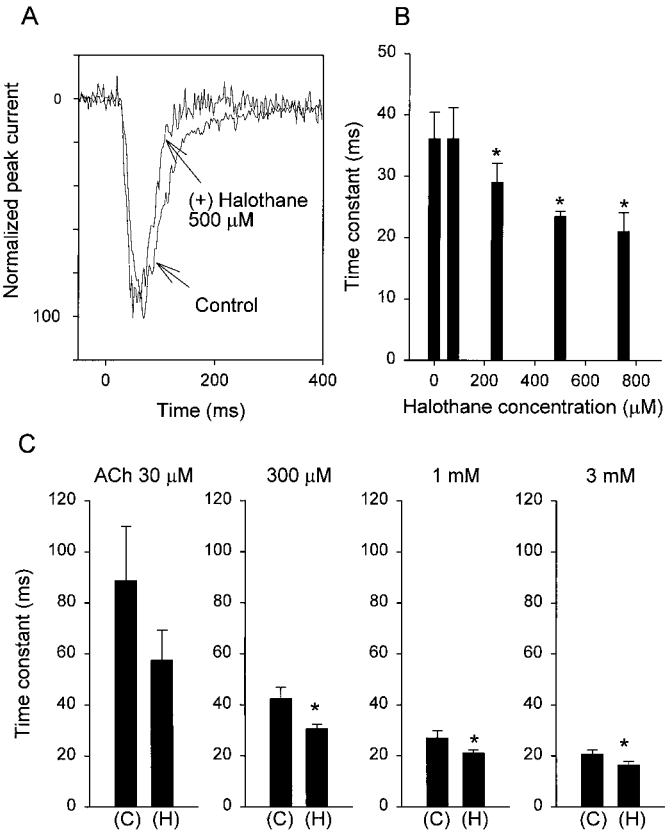

Fig. 4. Halothane acceleration of the decay phase of $\alpha7$-type currents. A, the peak of the currents in the absence and presence of 500 μM halothane was normalized to the same amplitude to compare the decay phase of $\alpha7$-type currents. B, halothane at 250, 500, and 750 μM significantly and concentration dependently shortened the decay time constant which was obtained by fitting the current with a single exponential function ($n = 5$, $p < 0.05$). C, halothane significantly shortened the decay time constant at any concentrations of ACh tested ($n = 5$, $p < 0.05$).

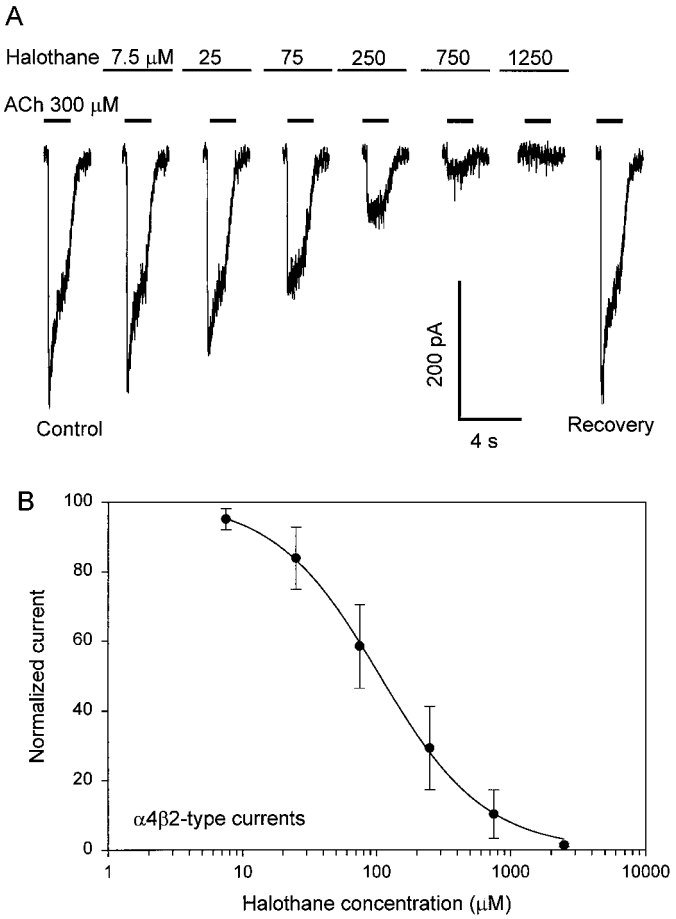

Fig. 5. Halothane block of $\alpha4\beta2$-type currents. A, halothane inhibited the currents induced by 300 μM ACh in a concentration-dependent manner. The inhibition was reversible after washout of halothane. B, concentration-response curve for halothane inhibition. The data points are the mean peak currents expressed as percentages of control current, and the error bars are standard deviations ($n = 10$). The line is unweighted least-squares fit of the data to a Hill equation. The IC_{50} and Hill coefficient obtained from halothane inhibition curve were 105 $\pm$ 7.0 μM and 1.10 $\pm$ 0.06, respectively.

halothane. Current 2 was generated when halothane was preperfused and also coapplied with ACh during test pulse. Preperfused halothane inhibited initial peak currents. This inhibition was removed by halothane-free ACh solution (current 1) exhibiting the time-dependent rise to the control level with a time constant of 285 ± 51 ms, which was significantly faster than halothane dissociation from the resting state ($p < 0.05$).

To monitor recovery from receptor desensitization, a high concentration of ACh (1 mM) was applied for 10 s to induce desensitization and its recovery was tested by a short test ACh pulse (Fig. 11B). The time course of the recovery of the receptor from the ACh-induced desensitization was 5.65 ± 0.29 s, a time much longer than the recovery from halothane block. This suggests that halothane inhibition of receptor is not caused by receptor desensitization.

Effects of Unstirred Layers on Rates of Halothane Blocking Action. The similarity between the onset of block of the resting receptor and the activated receptor made us to suspect that the onset of action might be rate-limited by solution exchange because of an unstirred layer surrounding the cell.

To examine the effect of unstirred layers on the drug action, the experiment protocol of Liu and Dilger (1991) was adapted here to determine solution exchange within the unstirred layer. As shown in Fig. 12, the patch electrode was capable of detecting junction potential change with a rise of time of 60 ms and in response to half-Na solution ACh current exhibited a peak before settling at the steady-state level within 215 ms. The transient peak has been attributed to a delay of solution exchange because of the effect of the unstirred layer. Thus, the onset and offset rate of halothane action was largely rate-limited by solution exchange because the onset time constants were similar to that for solution exchange. Thus, it is entirely possible that a fast open channel block could cause the resting receptor block and activated receptor block. The simulation based on such a notion could indeed reproduce the major effects of halothane on ACh dose-response curve, desensitization, and chlorisondamine open channel block (see *Discussion*).

Interaction of Halothane with Chlorisondamine. To get insight into the nature of halothane block of the $\alpha4\beta2$-type receptors, we studied the interaction of halothane with chlorisondamine. Chlorisondamine (Tocris Cookson Inc., Ballwin, MO) is an irreversible open channel blocker of nAChRs of frog muscle (Neely and Lingle, 1986), sympathetic ganglia (Rogers et al., 1997), and nnAChRs expressed in *X.*

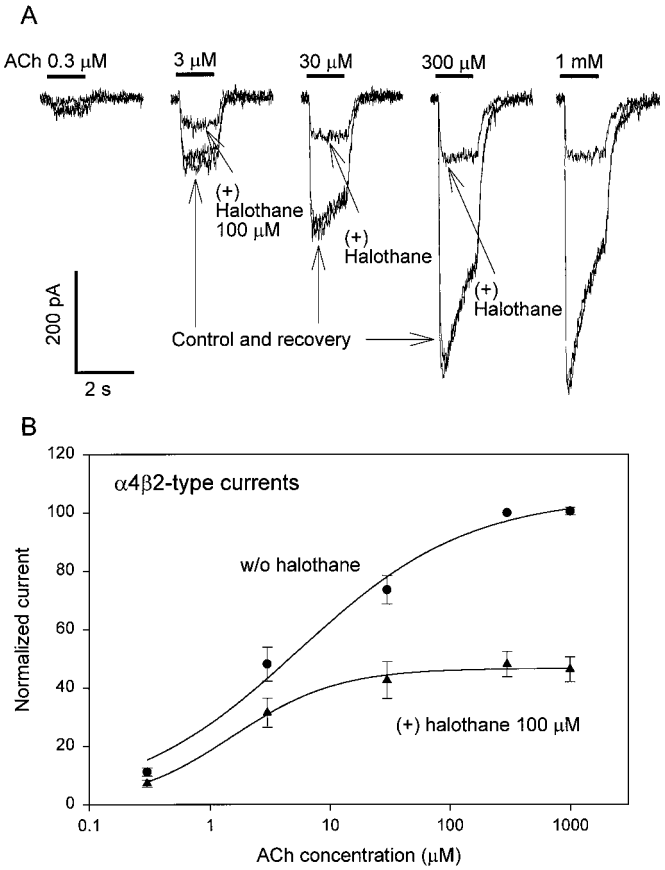

Fig. 6. Halothane block of $\alpha4\beta2$-type currents as a function of ACh concentration. A, halothane at 100 μM reversibly inhibited $\alpha4\beta2$-type currents at all ACh concentrations tested. The inhibition was slightly larger at high concentrations of ACh. B, ACh concentration-response curves in the absence and presence of 100 μM halothane. The data points are the mean peak currents expressed as percentages of control current, and the error bars are standard deviations ($n = 10$). The lines are unweighted least-squares fit of the data to a Hill equation. Halothane reduced the ACh EC_{50} value from 5.46 ± 2.40 μM to 1.53 ± 0.25 μM and increased the Hill coefficient from 0.61 ± 0.14 to 0.99 ± 0.14. Both changes are significant at a p value of < 0.05.

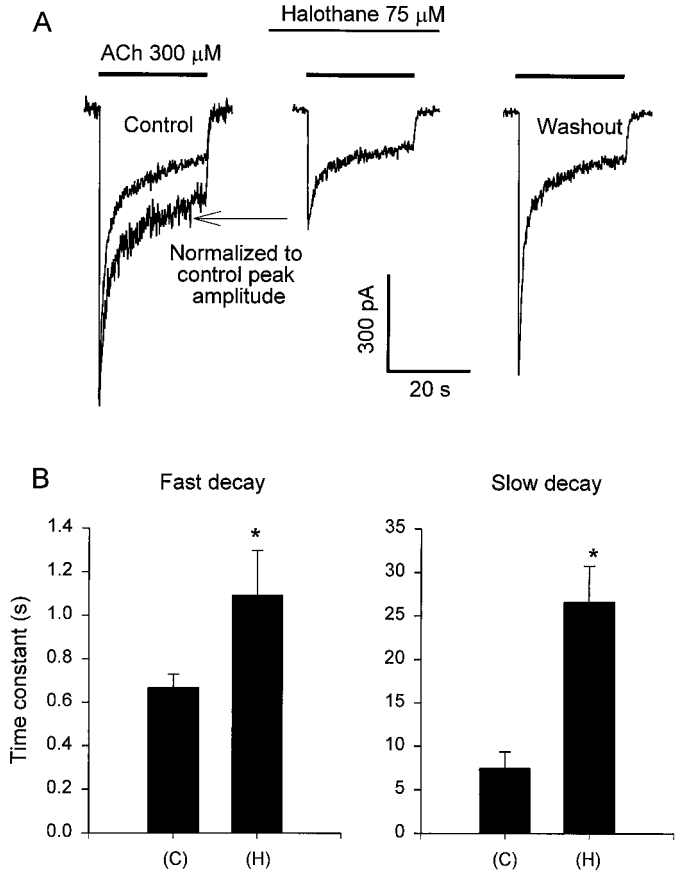

Fig. 7. Halothane effect on the decay phase of $\alpha4\beta2$-type currents. A, ACh 300 μM was applied for 25 s and the current was reversibly reduced in the presence of 75 μM halothane. The current in the presence of halothane was normalized to control peak and superimposed with control current. The decay could be well fit with a double exponential function. B, halothane increased both fast and slow decay time constants significantly ($n = 5$, $p < 0.05$).

laevis oocytes (Colquhoun and Patrick, 1997a). When 3 μM chlorisondamine was coapplied with 300 μM ACh for 3 s, the decay of ACh-induced current was greatly accelerated indicating open channel block (Fig. 13A). After 3 to 5 min of washout of chlorisondamine, the current was significantly reduced, indicating that chlorisondamine block was almost irreversible. In the presence of 250 μM and 750 μM halothane, however, the current after washout of halothane and chlorisondamine was larger than the control group (Fig. 13, B and C versus A). The current amplitude after washout was normalized to the control and is plotted as a function of halothane concentration (Fig. 13D). The fraction of receptor not blocked by chlorisondamine was significantly increased with an increase in halothane concentration. The halothane protection could be overcome by increasing chlorisondamine concentration. The protection by 750 μM halothane was drastically reduced when chlorisondamine was increased from 3 to 10 μM. These results suggest that halothane competitively protects the α4β2-type receptor from chlorisondamine block.

The decay phase accelerated by chlorisondamine coapplication was compared in the absence and presence of 250 μM halothane (Fig. 14). The chlorisondamine-induced acceleration of decay was slowed in the presence of halothane (Fig. 14A). The decay could be fit with a single exponential function, and the time constant was significantly increased in the presence of halothane (Fig. 14B). These results are consistent with a model in which the receptor can be blocked by either halothane or chlorisondamine. Halothane blocks and unblocks the open state of α4β2-type receptors more quickly than chlorisondamine does. Consequently, the halothane-blocked receptors became a sink for ACh receptors initially and became a source for chlorisondamine block as the open channels are depleted because of chlorisondamine block. Again, a simulation based on a simplified scheme will illustrate this point under *Discussion*.

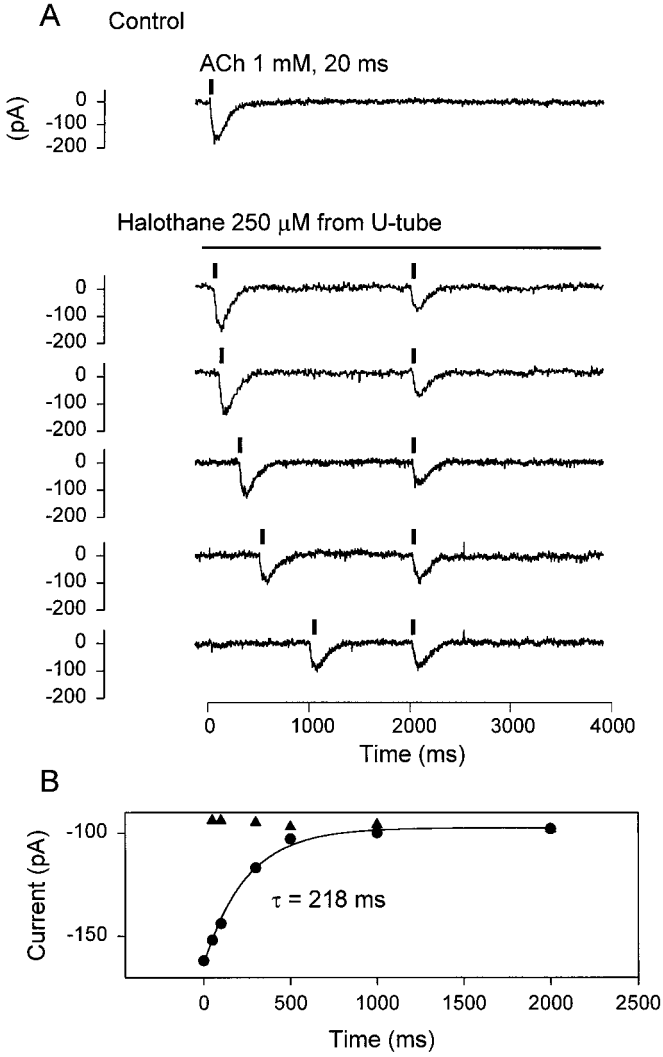

Fig. 8. Time course of halothane block of the resting α4β2-type receptor. A, ACh 1 mM was applied from a Picospritzer as test pulse and 250 μM halothane was applied from a U-tube onto the cell. Halothane was washed out between trials. To evaluate the resting channel block, the time to the first test pulse from the beginning of halothane application was varied in each trial. A second pulse was applied 2 s after the onset of halothane application to monitor the stability of the response. B, plot of the currents (●) as a function of the period of halothane perfusion shows that halothane inhibition of the resting α4β2-type receptor developed with a time constant of 218 ±18 ms (n = 4). Second pulse currents (▲) and their constant amplitude suggests halothane block is complete within 2 s.

Discussion

The present study demonstrated that halothane reversibly inhibited both α7-type and α4β2-type currents of nnAChRs in a concentration-dependent manner at clinically relevant concentrations. Furthermore, halothane block of α7-type currents was independent of ACh concentration, whereas the block of α4β2-type currents became less with decreasing ACh concentration.

The decay phases of α4β2-type and α7-type currents were differentially affected by halothane. Halothane accelerated the decay phase of α7-type currents while slowing the decay of α4β2-type currents (Figs. 4 and 7). This acceleration of the

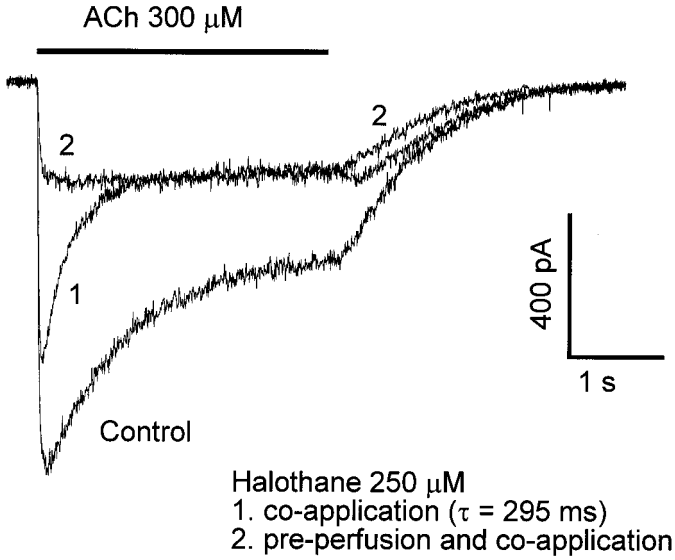

Fig. 9. Time course of halothane block of the activated α4β2-type receptor. Three currents induced by 300 μM ACh recorded in the same cell are superimposed. Control current was recorded in the absence of halothane. Current 1 was recorded when 250 μM halothane was coapplied with 300 μM ACh. Current 2 was recorded when 250 μM halothane was preperfused and coapplied with 300 μM ACh. When halothane was coapplied with ACh, the current exhibited time-dependent decay reaching the same level as that achieved by a combination of preperfusion and coapplication. This suggests that halothane has the same affinity for the resting state of receptor as well as for the activated receptor. The decay time constant estimated from current 1 was 295 ± 25 ms (n = 6).

decay phase of the α7-type currents suggest that halothane accelerates desensitization or causes open channel block. However, the fact that the halothane block of α7-type currents is independent of ACh concentration is not consistent with open channel block. On the other hand, halothane block of $\alpha4\beta2$-type currents is dependent on ACh concentration, suggesting open channel block. The ACh concentration-dependent block of $\alpha4\beta2$-type currents will be addressed later under *Discussion*.

Evidence has been obtained in support of the notion that general anesthetics directly act on ion channel proteins (Dilger et al., 1994; Forman et al., 1995; Eckenhoff, 1996). The M2 domain of $\alpha4\beta2$-type nnAChRs could be the site of halothane binding as suggested by Forman et al. (1995), who showed in mutagenesis experiments with muscle type nAChRs that anesthetics act on a specific amino acid in the M2 hydrophobic region that forms the pore lining. It is interesting to note that the N-terminal domain of α7 receptor outside the membrane was shown to be important for the inhibitory action of inhalational anesthetics using chimeric receptors (Zhang et al., 1997).

We have also found that halothane caused a shift in the ACh dose-response curve of $\alpha4\beta2$-type currents and protected the receptor from another open channel blocker, chlorisondamine. The experimental protocol failed to show unequivocally that halothane acts on the resting $\alpha4\beta2$-type nnAChRs as well as the activated receptors as was seen in muscle type nAChRs (Dilger et al., 1993, 1994; Wachtel, 1995; Scheller et al., 1997), because halothane blocked and unblocked the activated and resting receptors at the rates similar to that of solution exchanges in the unstirred layer. The time constants of the isoflurane binding to and unbinding from the muscle type nAChRs were estimated to be

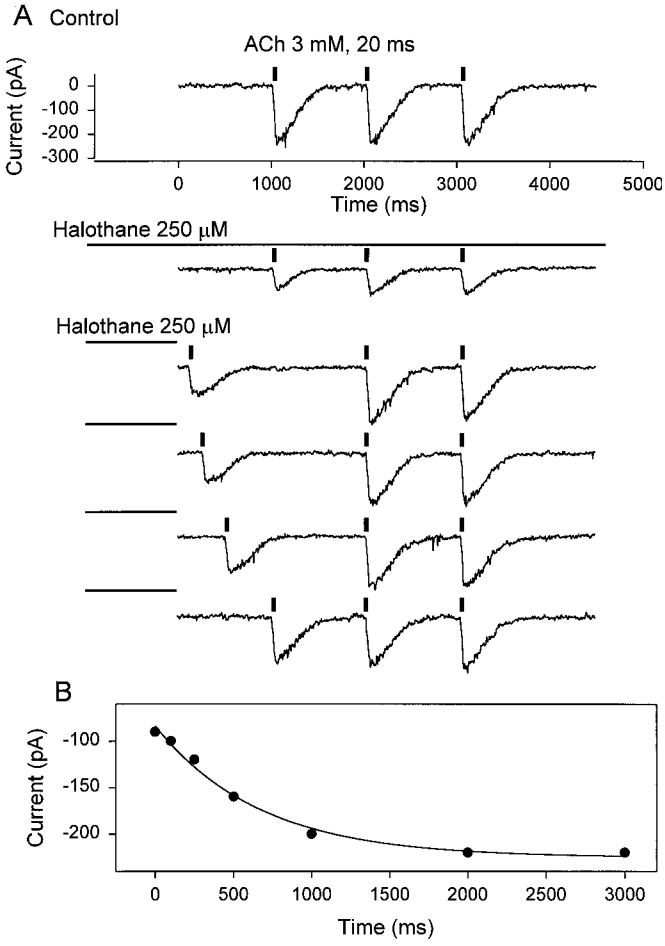

Fig. 10. The time course of recovery from halothane block in the resting $\alpha4\beta2$-type receptors. ACh 3 mM was applied from a Picospritzer and halothane 250 μM was applied in the bath. To observe recovery of the resting receptor, halothane was washed out by halothane-free solution from a U-tube. The time to the first test pulse from the beginning of washout was varied in each set of trial. Second and third pulses were applied 2 and 3 s after the onset of washout, respectively. The current recovered almost completely from halothane block in 2 s. Plot of the first pulse current as a function of the period of halothane washout shows that the recovery from halothane inhibition of the resting $\alpha4\beta2$-type receptor is time dependent (B) with a time constant of 499 $\pm$ 68 ms (n = 4).

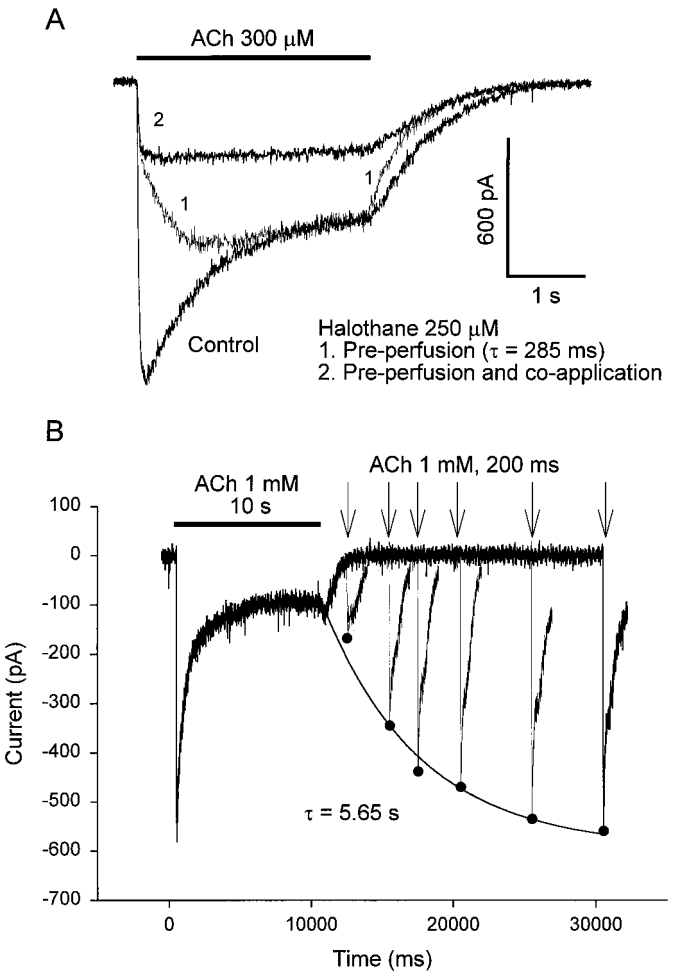

Fig. 11. Comparison of the recovery from halothane block in the $\alpha4\beta2$-type receptor during receptor activation with the recovery from receptor desensitization. A, three currents evoked by 300 μM ACh are superimposed. Control current was recorded in the absence of halothane. Current 1 was recorded when halothane was only preperfused 2 min before ACh test pulse which did not contain halothane. Current 2 was recorded when halothane was preperfused and also coapplied during test pulse. Preperfused halothane inhibited initial peak current. This inhibition was removed by halothane-free ACh solution exhibiting the time-dependent rise to the control level with a time constant of 285 $\pm$ 51 ms (n = 7). B, ACh-induced desensitization of the $\alpha4\beta2$-type receptor. A high concentration of ACh (1 mM) was applied for 10 s through a U-tube to induce receptor desensitization. The recovery of the $\alpha4\beta2$-type receptor from desensitization was monitored by applying ACh test pulses (1 mM). The time constant of the recovery of the $\alpha4\beta2$-type receptor from desensitization was 5.65 $\pm$ 0.29 s (n = 6) which was much longer than that of recovery from the halothane block.

around 500 μs using a rapid perfusion technique (Dilger et al., 1993). Direct modulation of $GABA_A$ receptors by halothane has recently been reported to occur within milliseconds (Li and Pearce, 2000). Thus, it is entirely possible that the resting block observed here is caused by a fast open channel block as seen with the muscle type nAChRs (Dilger et al., 1993).

Simulation of Halothane Effects on α4β2-Type nnAChRs. In the present study with the α4β2-type nnAChRs, halothane caused a shift in the ACh dose-response curve, slowed desensitization and protected the receptor from another open channel blocker, chlorisondamine. All of these halothane effects can be simulated by a simple model in which halothane rapidly blocks nnAChRs in the open state. In addition, the halothane-blocked receptor undergoes little or no desensitization. In the following simulation, we use a conventional scheme for the activation of nnAChRs. To simplify the simulation, we assume that the activated receptor undergoes desensitization and the halothane-bound and chlorisondamine-bound ones do not.

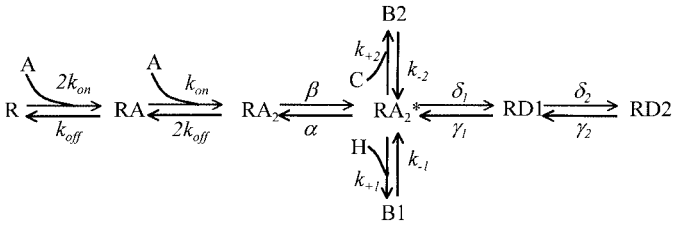

R is nnAChR, A is ACh, RA_2* is an open state, RD1 is a fast desensitized state, RD2 is a slow desensitized state, H is halothane, B1 is a halothane blocked state, C is chlorisondamine, and B2 is a chlorisondamine blocked state. Halothane is assumed to interact rapidly with the open state of the receptor.

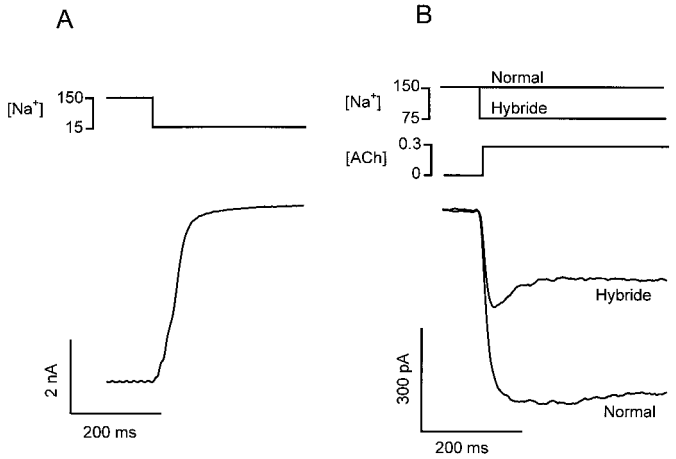

Fig. 12. Rate of solution exchange via the U-tube perfusion. A, the junction potential change in response to U-tube application of 15 mM Na^+ solution to a 150 mM Na^+ bathing solution was detected by a patch electrode with a rise time of 66.6 ± 3.30 ms (n = 5). B, ACh currents induced by the U-tube application of 0.3 mM ACh in 150 mM Na^+ solution rose with a rise time of 65.4 ± 2.20 ms (n = 6). When 0.3 mM ACh was applied via the U-tube containing 75 mM Na^+ solution to the cell bathing in 150 mM Na^+ containing solution (hybrid), ACh current rose to the peak before settling to a steady-state level, which was about 50% of the current recorded when both the bathing solution and the U-tube solution contained 150 mM Na^+. The settling times of 215 ± 30.0 ms (n = 5) arose from the effect of unstirred layers.

Effects of Halothane on Activation and Desensitization. Halothane modified ACh activation by shifting the ACh dose-response relationship in the direction of lower ACh concentration and by increasing the Hill coefficient. Such changes in activation could be largely accounted for by simulation of halothane block of the open channel (Fig. 15A). At high ACh concentrations, almost all receptors enter the open

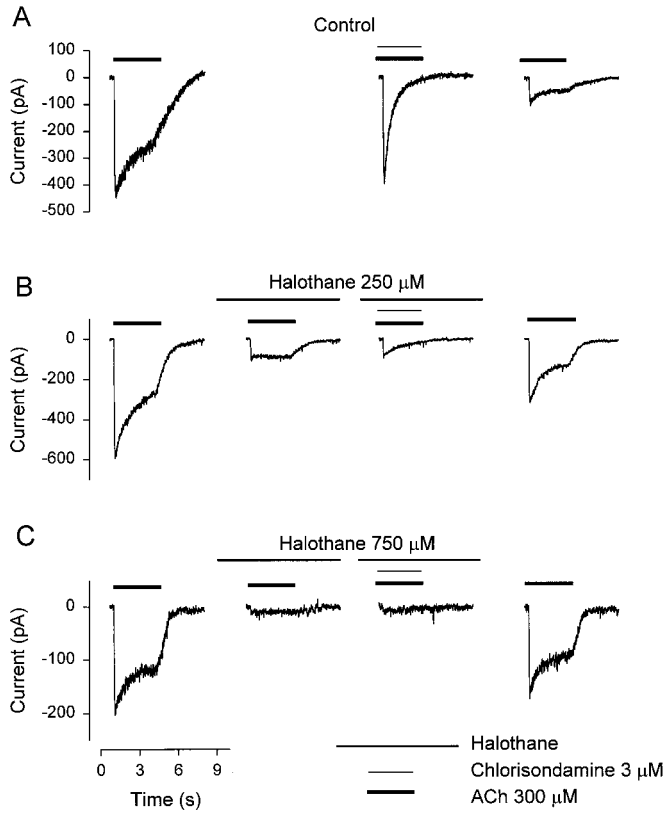

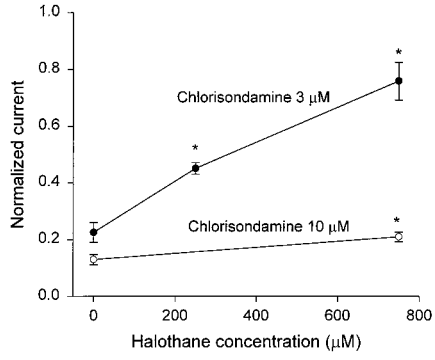

Fig. 13. Interaction of halothane with the open channel blocker chlorisondamine. A, currents were induced by 300 μM ACh for 3 s. After control recording, 3 μM chlorisondamine was coapplied with ACh. The decay of ACh-induced current was greatly accelerated suggesting open channel block. After 3 to 5 min of washout of chlorisondamine, the current was significantly reduced indicating that chlorisondamine block was almost irreversible. B and C, in the presence of halothane, the current after washout of halothane and chlorisondamine was larger than the control group in A. D, the current amplitude after washout was normalized to the control and is plotted as a function of halothane concentration. The fraction of unblocked receptor was significantly increased with an increase in halothane concentration (n = 8–12). The protection by 750 μM halothane was decreased with an increase in chlorisondamine concentration.

state, and the steady-state block by halothane is governed by the blocking and unblocking rate constants. At lower ACh concentrations (e.g., 10 μM), about 50% of the receptors that have entered the open state can be blocked rapidly by halothane. Because of this redistribution of the open state into conducting and blocked states, the transiently depleted conducting pool is replenished by converting more R to R2A*. The percentage of the blocked state is no longer determined solely by the blocking and unblocking rate constants. Consequently, less block is seen at lower ACh concentrations displaying a left shift in the ACh dose-response curve.

Simulation of Apparent Slowing in Desensitization. Halothane slowed current decay during a prolonged application of 300 μM ACh, which might be construed as indicative of slowing of receptor desensitization. In the simulation of the effect of halothane in slowing the ACh current decay, we have to assume that the halothane-blocked receptors undergo little or no desensitization. In the simulation shown in Fig. 15B, the halothane-bound receptor was assumed not to undergo desensitization. After the application of 300 μM ACh without halothane, the receptors enter the conducting state rapidly, and then decayed slowly. The kinetics of current decay are indicative of receptor desensitization and are determined by forward and backward rate constants governing the transition into two desensitized states. The slowing of current decay in the presence of 75 μM halothane could be simulated by the above kinetic scheme on the assumption that about 50% of the receptors are rapidly blocked by halothane without undergoing desensitization whereas the rest undergo normal desensitization. The halothane-blocked state initially serves as current sink and later becomes current source. Under this condition, the current decay is no longer

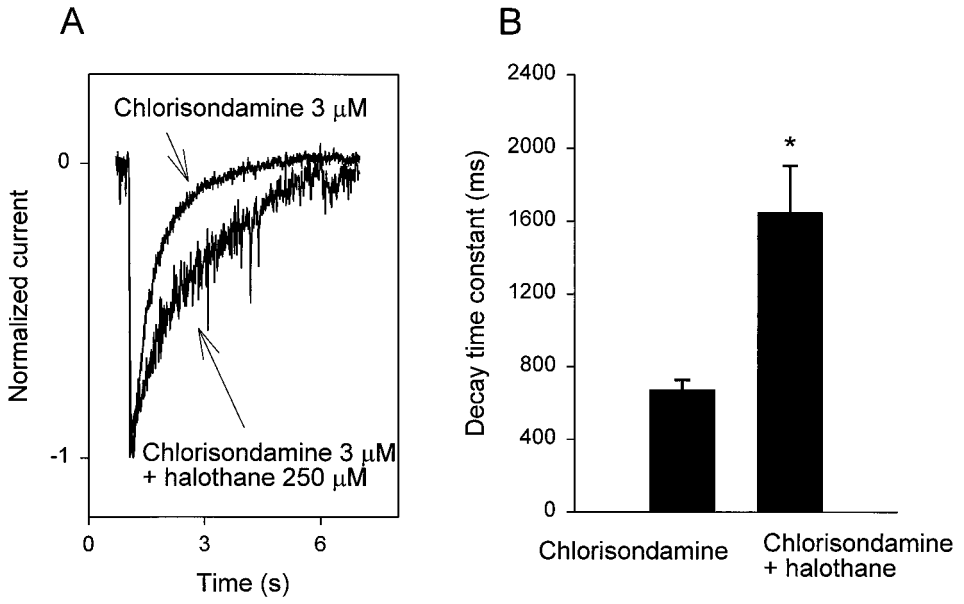

Fig. 14. Halothane 250 μM slows the current decay accelerated by 3 μM chlorisondamine. A, to facilitate the comparison of the decay phases, the peak current in the presence of 250 μM halothane was normalized to the control. Chlorisondamine-induced acceleration of the decay was slowed by halothane. B, the decay phase was fit with a single exponential function to calculate the decay time constant which was significantly increased in the presence of halothane (n = 9–12) ($p < 0.05$).

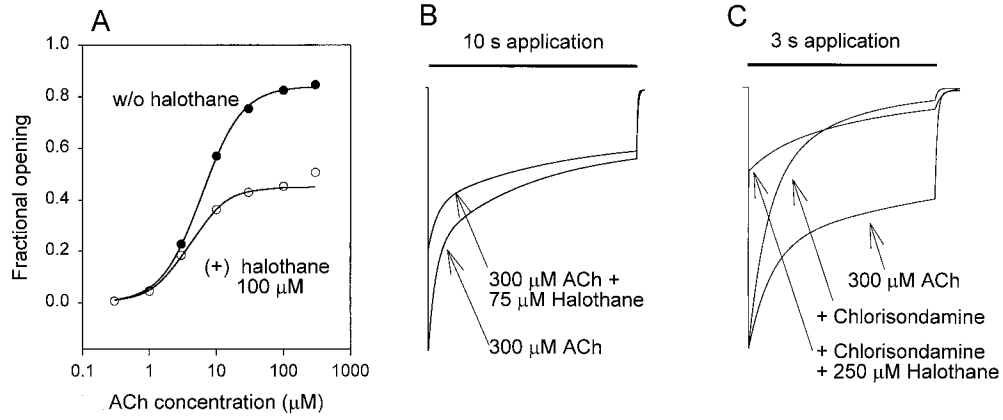

Fig. 15. Simulation of the effects of halothane on ACh concentration-response relathionship, desensitization, and chlorisondamine block. Numerical solution of the kinetic Scheme 1 was carried out with C++ program. The following rate constants were used: $k_{on} = 1 \times 10^7$ M^{-1} s^{-1}, $k_{off} = 100$ s^{-1}, $\beta = 3000$ s^{-1}, $\alpha = 500$ s^{-1}, $\delta_1 = 1.4$ s^{-1}, $\gamma_1 = 1.4$ s^{-1}, $\delta_2 = 0.28$ s^{-1}, $\gamma_2 = 0.084$ s^{-1}, $k_{+1} = 1 \times 10^7$ M^{-1} s^{-1}, $k_{-1} = 1 \times 10^3$ s^{-1} for governing halothane block, $k_{+2} = 5 \times 10^6$ M^{-1} s^{-1}, $k_{-2} = 0.01$ s^{-1} for governing chlorisondamine block. A, symbols are simulated data fitted with the Hill equation. Halothane at 100 μM decreased the EC_{50} value for ACh from 6.08 μM to 3.95 μM and increased the Hill coefficient from 1.44 to 1.54. B, ACh current peaked rapidly and was followed by two phases of decay during a prolonged application of 300 μM ACh. In the presence of 75 μM halothane, the peak was reduced and current decay was slowed. The fast time constant was increased from 0.4 to 0.8 s and the slow time constant was increased from 5 to more than100 s. C, halothane protects the receptor from chlorisondamine block. In the presence of 3 μM chlorisondamine, the ACh current induced by 300 μM ACh reached the peak rapidly and then decayed with a time constant of 515 ms. The decay phase was slowed by 250 μM halothane with a decay time constant of 1.28 s. At the end of 3 s, 3 μM blocked 80% of the receptors in the control and 60% of the receptors in the presence of 250 μM halothane as seen experimentally (Fig. 13D).

determined solely by the rate constants governing the desensitization step and is influenced by the late arrival of conducting state from the blocked state.

Halothane Protects Receptors from Chlorisondamine Block. Halothane decreased the chlorisondamine block of $\alpha4\beta2$-type receptors in a concentration-dependent manner. This suggests that halothane somehow prevents chlorisondamine from binding to the open receptor channel. In the simulation of competitive block of open channels by halothane and chlorisondamine, we added a chlorisondamine-blocked state, B2, with forward and backward rate constants governing its block. As shown in Fig. 15C, chlorisondamine at 3 μM blocked the receptor with a time constant of 600 ms to 20% of the control. In the presence of 250 μM halothane, block by 3 μM chlorisondamine became slower and its time constant was increased to 1.87 s from the control of 0.60 s. Mechanistically, the slowing in the current decay is caused by the late arrival of the conducting state from the halothane-bound state. In addition, only 40% of the receptors are blocked by chlorisondamine because fewer receptors are available due to competitive block by halothane.

Comparison with Previous Results. The results of the present experiments with the nnAChRs of rat cortical neurons may be compared with those with the chicken receptors expressed in *X. laevis* oocytes (Flood et al., 1997). Halothane and isoflurane both potently inhibit the $\alpha4\beta2$-type current with similar IC_{50} values (105 μM or 0.4 MAC for halothane and 85 μM or 0.3 MAC for isoflurane). However, their block differs in the ACh concentration dependence. Halothane block increases with ACh concentration, where isoflurane block decreases. The $\alpha7$-type receptor is much less sensitive to the anesthetics than the $\alpha4\beta2$-type receptor. Halothane at 552 μM (2.2 MACs) inhibits the $\alpha7$-type current 50% whereas isoflurane at 640 μM (2 MACs) has no effect. These differences may be attributed to different expression systems (native cortical neurons versus *X. laevis* oocytes) and/or different animal species (rat versus chicken).

Violet et al. (1997) also studied the effect of halothane on nnAChRs expressed in *X. laevis* oocytes. They found that the halothane IC_{50} value for the $\alpha4\beta2$ receptor expressed in oocytes was 27 μM compared with 105 μM in the present study. In contrast to our finding, they found that halothane block was independent of ACh concentration. Because the source of material (rat) is the same in both studies, the quantitative differences must be caused by the different expression system. Consistent with this view are the findings that the ACh EC_{50} value for the rat $\alpha4\beta2$ receptor is estimated to be 104 μM (Violet et al., 1997), whereas the value for the $\alpha4\beta2$-type current of native rat cortical neurons is 3 μM (Aistrup et al., 1999) or 5.5 μM (present study).

The time constant for the recovery of the $\alpha4\beta2$-type nnAChR currents from halothane block (<300 ms) was much faster than the recovery from ACh-induced desensitization (5.65 s). This strongly suggests that halothane block is not caused by desensitization. The above simulation also suggests that the halothane-bound receptor might not undergo desensitization at all. This is in contrast with studies with the muscle type nAChRs. Several studies have suggested that general anesthetics stabilize the slowly desensitized conformational state in the muscle type nAChRs through conversion from a low-affinity state to a high-affinity state by agonist (Young and Sigman, 1983; Dilger et al., 1993; Firestone et al., 1994; Raines et al., 1995). In addition, Violet et al. (1997) found that the muscle nAChRs are 32 times less sensitive to halothane than the $\alpha4\beta2$ nnAChRs.

Clinical Implication of Potent Effect of Halothane on nnAChRs. There is general agreement that nnAChRs located in presynaptic and preterminal sites modulate the release of various neurotransmitters such as norepinephrine, dopamine, GABA, glutamate, serotonin, and ACh itself (Role and Berg, 1996; Alkondon et al., 1997, 1999; Wonnacott, 1997). Along this line, several studies demonstrated that the modulation of neurotransmitter release mediated by nnAChRs was affected by inhalational anesthetics. At clinically relevant concentrations, inhalational anesthetics suppressed nicotine-induced dopamine release in rat striatum (Salord et al., 1997), nicotine-induced catecholamine release in chromaffin cells (Sumikawa et al., 1982; Pocock and Richards, 1988), and ACh release in rat striatum and cerebral cortex (Shichino et al., 1998). Thus, the inhibition of nnAChRs by halothane observed in the present study could potently modulate the neurotransmitter release in the central nervous system. Our preliminary experiments using cortical neurons in long-term culture showed that the increase in the frequency of miniature excitatory postsynaptic currents by exogenously administered ACh in the presence of tetrodotoxin was inhibited by halothane without change in the amplitude.

Halothane reversibly inhibited both $\alpha7$-type and $\alpha4\beta2$-type currents of nnAChRs with IC_{50} values of 552 and 105 μM, respectively. The IC_{50} value for $\alpha4\beta2$-type currents is a subanesthetic concentration and almost equivalent to 0.4 MAC, whereas the IC_{50} value for $\alpha7$-type currents is more than surgical concentration and almost equivalent to 2 MACs. Thus, the $\alpha4\beta2$-type receptors in rat cortical neurons are highly sensitive to halothane and may play an important role for clinical anesthesia, whereas the $\alpha7$-type receptors may be less significant for anesthesia.

At subanesthetic doses, inhalational anesthetics have been shown to induce diverse behavioral effects, including suppression of learning and memory (Newton et al., 1990, Galinkin et al., 1997; Dwyer et al., 1992), drowsiness (Newton et al., 1990; Galinkin et al., 1997), and cognition impairment (Galinkin et al., 1997). ACh is one of the important neurotransmitters released from the brain stem, hypothalamus, basal forebrain, cerebral cortex that participate in cognition, memory, learning, alertness, and antinociception (McCormick and Bal, 1997; Changeux et al., 1998). Suppression of interneuronal activity in cerebral cortex is suspected to play an important role for primary hypnotic action of anesthetics (Woodforth et al., 1999). This suggests that drowsiness and unconsciousness caused by inhalational anesthetics may be caused, at least in part, by suppression of cerebral cortex. Thus the high sensitivity of nnAChRs, α-BuTX-insensitive $\alpha4\beta2$-type receptors in particular, to halothane in interneurons of cerebral cortex may explain various behavioral effects of anesthetics such as hypnosis, amnesia, cognition impairment, and drowsiness.

In summary, halothane block of the $\alpha4\beta2$-type nnAChRs at subanesthetic and anesthetic concentrations is deemed to play an important role in anesthesia via a direct action on the receptor and an indirect action to suppress release of various neurotransmitters.

Acknowledgments

We thank Nayla Hasan for technical assistance and Julia Irizarry for secretarial assistance.

References

Aistrup GL, Marszalec W and Narahashi T (1999) Ethanol modulation of nicotinic acetylcholine receptor currents in cultured cortical neurons. *Mol Pharmacol* **55:** 39–49.

Albuquerque EX, Alkondon M, Pereira EF, Castro NG, Schrattenholz A, Barbosa CT, Bonfante-Cabarcas R, Aracava Y, Eisenberg HM and Maelicke A (1997) Properties of neuronal nicotinic acetylcholine receptors: Pharmacological characterization and modulation of synaptic function. *J Pharmacol Exp Ther* **280:**1117–1136.

Alkondon M, Pereira EF, Barbosa CT and Albuquerque EX (1997) Neuronal nicotinic acetylcholine receptor activation modulates γ-aminobutyric acid release from CA1 neurons of rat hippocampal slices. *J Pharmacol Exp Ther* **283:**1396–1411.

Alkondon M, Pereira EF, Eisenberg HM and Albuquerque EX (1999) Choline and selective antagonists identify two subtypes of nicotinic acetylcholine receptors that modulate GABA release from CA1 interneurons in rat hippocampal slices. *J Neurosci* **19:**2693–2705.

Cardoso RA, Yamakura T, Brozowski SJ, Chavez-Noriega LE and Harris RA (1999) Human neuronal nicotinic acetylcholine receptors expressed in *Xenopus* oocytes predict efficacy of halogenated compounds that disobey the Meyer-Overton rule. *Anesthesiology* **91**:1370–1377.

Changeux JP, Bertrand D, Corringer PJ, Dehaene S, Edelstein S, Lena C, Le Novere N, Marubio L, Picciotto M and Zoli M (1998) Brain nicotinic receptors: Structure and regulation, role in learning and reinforcement. *Brain Res Brain Res Rev* **26:**198–216.

Colquhoun LM and Patrick JW (1997a) α3, β2, and β4 form heterotrimeric neuronal nicotinic acetylcholine receptors in *Xenopus* oocytes. *J Neurochem* **69**:2355–2362.

Colquhoun LM and Patrick JW (1997b) Pharmacology of neuronal nicotinic acetylcholine receptor subtypes. *Adv Pharmacol* **39:**191–220.

Cooper ST and Millar NS (1997) Host cell-specific folding and assembly of the neuronal nicotinic acetylcholine receptor α7 subunit. *J Neurochem* **68:**2140–2151.

Dilger JP, Brett RS and Mody HI (1993) The effects of isoflurane on acetylcholine receptor channels.: 2. Currents elicited by rapid perfusion of acetylcholine. *Mol Pharmacol* **44:**1056–1063.

Dilger JP, Vidal AM, Mody HI and Liu Y (1994) Evidence for direct actions of general anesthetics on an ion channel protein. A new look at a unified mechanism of action. *Anesthesiology* **81:**431–442.

Dwyer R, Bennett HL and Eger EI 2nd (1992) Heilbron D. Effects of isoflurane and nitrous oxide in subanesthetic concentrations on memory and responsiveness in volunteers. *Anesthesiology* **77:**888–898.

Eckenhoff RG (1996) An inhalational anesthetic binding domain in the nicotinic acetylcholine receptor. *Proc Natl Acad Sci USA* **93:**2807–2810.

Firestone LL, Alifimoff JK and Miller KW (1994) Does general anesthetic-induced desensitization of the *Torpedo* acetylcholine receptor correlate with lipid disordering? *Mol Pharmacol* **46:**508–515.

Flood P, Ramirez-Latorre J and Role L (1997) α4β2 neuronal nicotinic acetylcholine receptors in the central nervous system are inhibited by isoflurane and propofol, but α7-type nicotinic acetylcholine receptors are unaffected. *Anesthesiology* **86:** 859–865.

Forman SA, Miller KW and Yellen G (1995) A discrete site for general anesthetics on a postsynaptic receptor. *Mol Pharmacol* **48:**574–581.

Franks NP and Lieb WR (1993) Selective actions of volatile general anaesthetics at molecular and cellular levels. *Br J Anaesth* **71:**65–76.

Franks NP and Lieb WR (1994) Molecular and cellular mechanisms of general anaesthesia. *Nature (Lond)* **367:**607–614.

Franks NP and Lieb WR (1996) Temperature dependence of the potency of volatile general anesthetics: Implications for in vitro experiments. *Anesthesiology* **84:**716–720.

Galinkin JL, Janiszewski D, Young CJ, Klafta JM, Klock PA, Coalson DW, Apfelbaum JL and Zacny JP (1997) Subjective, psychomotor, cognitive, and analgesic effects of subanesthetic concentrations of sevoflurane and nitrous oxide. *Anesthesiology* **87:**1082–1088.

Hamill OP, Marty A, Neher E, Sakmann B and Sigworth FJ (1981) Improved patch-clamp techniques for high-resolution current recording from cells and cell-free membrane patches. *Pfluegers Arch Eur J Physiol* **391:**85–100.

Kissin I (1993) General anesthetic action: An obsolete notion? *Anesth Analg* **76:**215–218.

Lewis TM, Harkness PC, Sivilotti LG, Colquhoun D and Millar NS (1997) The ion channel properties of a rat recombinant neuronal nicotinic receptor are dependent on the host cell type. *J Physiol* **505:**299–306.

Li X and Pearce RA (2000) Effects of halothane on $GABA_A$ receptor kinetics: Evidence for slowed agonist unbinding. *J Neurosci* **20:**899–907.

Lindstrom J (1996) Nicotinic acetylcholine receptors, in *Ion Channels*, Vol. 4. (Narahashi T eds) pp 377–450, Plenum Press, New York.

Lindstrom J (1997) Nicotinic acetylcholine receptors in health and disease. *Mol Neurobiol* **15:**193–222.

Liu Y and Dilger JP (1991) Opening rate of acetylcholine receptor channels. *Biophys J* **60:**424–432.

Marszalec W, Aistrup GL and Narahashi T (1998) Ethanol modulation of excitatory and inhibitory synaptic interactions in cultured cortical neurons. *Alcohol Clin Exp Res* **22:**1516–1524.

Marszalec W, Aistrup GL and Narahashi T (1999) Ethanol-nicotine interactions at α-bungarotoxin-insensitive nicotinic acetylcholine receptors in rat cortical neurons. *Alcohol Clin Exp Res* **23:**439–445.

Marszalec W and Narahashi T (1993) Use-dependent pentobarbital block of kainate and quisqualate currents. *Brain Res* **608:**7–15.

Marubio LM, del Mar Arroyo-Jimenez M, Cordero-Erausquin M, Lena C, Le Novere N, de Kerchove d'Exaerde A, Huchet M, Damaj MI and Changeux JP (1999) Reduced antinociception in mice lacking neuronal nicotinic receptor subunits. *Nature (Lond)* **398:**805–810.

McCormick DA and Bal T (1997) Sleep and arousal: Thalamocortical mechanisms. *Ann Rev Neurosci* **20:**185–215.

McGehee DS and Role LW (1995) Physiological diversity of nicotinic acetylcholine receptors expressed by vertebrate neurons. *Annu Rev Physiol* **57:**521–546.

McKenzie D, Franks NP and Lieb WR (1995) Actions of general anaesthetics on a neuronal nicotinic acetylcholine receptor in isolated identified neurones of *Lymnaea stagnalis*. *Br J Pharmacol* **115:**275–282.

Meyer H (1899) Zur Theorie der Alkoholnarkose. *Arch Exp Pathol Pharmakol* **42**: 109–118.

Nakahiro M, Yeh JZ, Brunner E and Narahashi T (1989) General anesthetics modulate GABA receptor channel complex in rat dorsal root ganglion neurons. *FASEB J* **3:**1850–1854.

Neely A and Lingle CJ (1986) Trapping of an open-channel blocker at the frog neuromuscular acetylcholine channel. *Biophys J* **50:**981–986.

Newton DE, Thornton C, Konieczko K, Frith CD, Dore CJ, Webster NR and Luff NP (1990) Levels of consciousness in volunteers breathing sub-MAC concentrations of isoflurane. *Br J Anaesth* **65:**609–615.

Pocock G and Richards CD (1988) The action of volatile anaesthetics on stimulus-secretion coupling in bovine adrenal chromaffin cells. *Br J Pharmacol* **95:**209–217.

Raines DE, Rankin SE and Miller KW (1995) General anesthetics modify the kinetics of nicotinic acetylcholine receptor desensitization at clinically relevant concentrations. *Anesthesiology* **82:**276–287.

Rogers M, Colquhoun LM, Patrick JW and Dani JA (1997) Calcium flux through predominantly independent purinergic ATP and nicotinic acetylcholine receptors. *J Neurophysiol* **77:**1407–1417.

Role LW and Berg DK (1996) Nicotinic receptors in the development and modulation of CNS synapses. *Neuron* **16:**1077–1085.

Salord F, Keita H, Lecharny JB, Henzel D, Desmonts JM and Mantz J (1997) Halothane and isoflurane differentially affect the regulation of dopamine and γ-aminobutyric acid release mediated by presynaptic acetylcholine receptors in the rat striatum. *Anesthesiology* **86:**632–641.

Scheller M, Bufler J, Schneck H, Kochs E and Franke C (1997) Isoflurane and sevoflurane interact with the nicotinic acetylcholine receptor channels in micromolar concentrations. *Anesthesiology* **86:**118–127.

Seto T, Mashimo T, Yoshiya I, Kanashiro M and Taniguchi Y (1992) The solubility of volatile anaesthetics in water at 25.0°C using ^{19}F NMR spectroscopy. *J Pharm Biomed Anal* **10:**1–7.

Shichino T, Murakawa M, Adachi T, Arai T, Miyazaki Y and Mori K (1998) Effects of inhalation anaesthetics on the release of acetylcholine in the rat cerebral cortex in vivo. *Br J Anaesth* **80:**365–370.

Sivilotti LG, McNeil DK, Lewis TM, Nassar MA, Schoepfer R and Colquhoun D (1997) Recombinant nicotinic receptors, expressed in *Xenopus* oocytes, do not resemble native rat sympathetic ganglion receptors in single-channel behaviour. *J Physiol* **500**:123–138

Smith RA, Porter EG and Miller KW (1981) The solubility of anesthetic gases in lipid bilayers. *Biochim Biophys Acta* **645:**327–338.

Stanski DR (1994) Monitoring depth of anesthesia, in *Anesthesia,* 4th ed (Miller RD eds) pp 1127–1160, Churchill Livingstone, New York.

Sumikawa K, Matsumoto T, Ishizaka N,Nagai H, Amenomori Y and Amakata Y (1982) Mechanism of the differential effects of halothane on nicotinic- and muscarinic-receptor-mediated responses of the dog adrenal medulla. *Anesthesiology* **57:** 444–450.

Violet JM, Downie DL, Nakisa RC, Lieb WR and Franks NP (1997) Differential sensitivities of mammalian neuronal and muscle nicotinic acetylcholine receptors to general anesthetics. *Anesthesiology* **86:**866–874.

Wachtel RE (1995) Relative potencies of volatile anesthetics in altering the kinetics of ion channels in BC3H1 cells. *J Pharmacol Exp Ther* **274:**1355–1361.

Wonnacott S (1997) Presynaptic nicotinic ACh receptors. *Trends Neurosci* **20:**92–98.

Woodforth IJ, Hicks RG, Crawford MR, Stephen JP and Burke D (1999) Depression of I waves in corticospinal volleys by sevoflurane, thiopental, and propofol. *Anesth Analg* **89:**1182–1187.

Yeh JZ, Quandt FN, Tanguy J, Nakahiro M, Narahashi T and Brunner EA (1991) General anesthetic action on γ-aminobutyric acid-activated channels. *Ann NY Acad Sci* **625:**155–173.

Young AP and Sigman DS (1983) Conformational effects of volatile anesthetics on the membrane-bound acetylcholine receptor protein: Facilitation of the agonist-induced affinity conversion. *Biochemistry* **22:**2155–2162.

Zhang L, Oz M, Stewart RR, Peoples RW and Weight FF (1997) Volatile general anaesthetic actions on recombinant nACh α7, 5-HT3 and chimeric nACh α7–5-HT3 receptors expressed in *Xenopus* oocytes. *Br J Pharmacol* **120**:353–355.

Send reprint requests to: Dr. Toshio Narahashi, Ph.D., Department of Molecular Pharmacology and Biological Chemistry, Northwestern University Medical School, 303 Chicago Avenue, Chicago IL. E-mail: tna597@northwestern.edu